BIODIVERSITAS
Volume 27, Number 3, March 2026
Pages: 17

ISSN: 1412-033X
E-ISSN: 2085-4722
https://doi.org/10.13057/biodiv/d270325

Exploration of bacterial communities for low-density polyethylene (LDPE) degradation in the mangrove area of Pamekasan, East Java, Indonesia

JUALITA FARADHA ACHNASYA[1] , ARTINI PANGASTUTI[1,2,♥], SITI LUSI ARUM SARI[2]

[1]Graduate Program of Bioscience, Faculty of Mathematics and Natural Sciences, Universitas Sebelas Maret. Jl. Ir. Sutami 36A, Surakarta 57126, Central Java, Indonesia. Tel.: +62-271-669376, Fax.: +62-271-663375, ♥email: artini_p@staff.uns.ac.id

[2]Department of Biology, Faculty of Mathematics and Natural Sciences, Universitas Sebelas Maret. Jl. Ir. Sutami 36A Surakarta 57126, Central Java, Indonesia

Manuscript received: 19 November 2025. Revision accepted: 20 March 2026.

Abstract. *Achnasya JF, Pangastuti A, Sari SLA. 2026. Exploration of bacterial communities for low-density polyethylene (LDPE) degradation in the mangrove area of Pamekasan, East Java, Indonesia. Biodiversitas 27 (3): d270325. https://doi.org/10.13057/biodiv/d270325.* Low-density polyethylene (LDPE) is one of the most widely used synthetic plastics and a major contributor to persistent pollution in coastal ecosystems, including mangrove environments. Mangroves act as natural sinks for plastic debris, yet the diversity and functional potential of plastisphere-associated bacteria in these systems remain insufficiently understood. This study investigated bacterial community dynamics during LDPE-driven enrichment and identified indigenous LDPE-degrading bacteria from mangrove sediments in Pamekasan, East Java, Indonesia. Sediment samples from three mangrove sites were subjected to three sequential enrichment cultures using carbon-free marine medium with LDPE beads as the sole carbon source. Microbial community shifts were analyzed through metagenomic sequencing, while LDPE degradation capacity was evaluated using gravimetric weight loss, FTIR spectroscopy, and SEM-EDX analyses. Enrichment resulted in pronounced restructuring of bacterial communities, characterized by reduced richness but increased functional specialization across culture stages. Dominant taxa included *Qipengyuania*, *Flavobacterium*, *Acinetobacter*, *Pseudoxanthomonas*, and *Pseudomonas*, with a stable core of ASVs persisting throughout enrichment. From the tertiary culture, three culturable isolates demonstrated LDPE-degrading potential: *Microbacterium aurantiacum* K2, *Microbacterium* sp. K3, and *Bacillus* sp. K5. Among these, *Bacillus* sp. K5 exhibited the highest degradation efficiency, achieving 21.35% LDPE weight loss, followed by Microbacterium sp. K3 (20.27%) and M. aurantiacum K2 (17.10%). FTIR and SEM analyses confirmed oxidative surface modification and structural damage of LDPE films. These findings demonstrate that mangrove plastisphere communities harbor specialized bacteria capable of initiating LDPE degradation and highlight the ecological role of enrichment-driven microbial selection. The study provides a foundation for developing nature-based and environmentally compatible strategies for mitigating plastic pollution in coastal ecosystems.

Keywords: Biodegradation, low-density polyethylene, mangrove ecosystems, metagenomic analysis, plastic-degrading bacteria

INTRODUCTION

Low-density polyethylene (LDPE) is one of the most widely produced synthetic polymers and constitutes a major contributor to persistent plastic pollution in aquatic and coastal environments (Geyer et al. 2017; Li et al. 2020). Its extensive application in single-use packaging, combined with inefficient waste management, has resulted in its widespread accumulation across marine ecosystems. Due to its high molecular weight, hydrophobic nature, and chemical stability, LDPE is highly resistant to natural degradation processes and can persist for extended periods in both sediments and water columns (Li et al. 2020). In low-energy environments, where hydrodynamic forces are limited, plastic debris is readily retained and subjected to gradual fragmentation, increasing its environmental persistence and ecological impact.

Mangrove ecosystems are particularly vulnerable to plastic accumulation. The complex root systems of mangroves, including pneumatophores and prop roots, facilitate the trapping and burial of plastic debris within sediments (Smith 2012). Consequently, mangrove forests function as effective sinks for both macroplastics and microplastics (Cordova et al. 2023). Prolonged accumulation of plastic materials can alter sediment physicochemical properties, limit oxygen diffusion, and reduce permeability, thereby disrupting microbial-mediated biogeochemical processes (Silva et al. 2021; Deakin et al. 2025). These disturbances may impair nutrient cycling, affect plant growth, and reduce the resilience of mangrove-associated biota. Indonesia, which hosts the largest mangrove area globally (UNEP 2021; Williams and Buitrago 2022), represents critical region for examining the environmental fate of plastics. Therefore, understanding degradation processes in mangrove ecosystems is essential for biodiversity conservation and sustainable coastal management.

In aquatic systems, plastic surfaces are rapidly colonized by diverse microbial communities known as the plastisphere (Zettler et al. 2013). These biofilm-forming assemblages differ from surrounding free-living microorganisms in both composition and ecological function (Wright et al. 2021). The plastisphere often includes taxa capable of adhering to

hydrophobic substrates and utilizing plastic-associated compounds. Within these biofilms, microorganisms produce oxidative and hydrolytic enzymes that modify polymer surfaces, promote chain scission, and generate low-molecular-weight compounds (Mohanan et al. 2020; Mishra et al. 2023). These compounds may subsequently serve as carbon and energy sources for microbial metabolism. Although LDPE is considered highly recalcitrant, increasing evidence indicates that naturally occurring microbial consortia can induce partial degradation under selective environmental conditions (Moharir and Kumar 2019; Wang et al. 2021).

Recent advances in high-throughput sequencing have enhanced the resolution of microbial community analyses in plastisphere studies. Amplicon sequence variant (ASV)-based approaches enable precise tracking of microbial succession during enrichment processes and allow identification of dominant and persistent taxa (Dhali et al. 2024). However, sequence-based approaches alone cannot directly confirm functional degradation capacity (Madhuri et al. 2019). In contrast, culture-dependent methods provide experimental validation of biodegradation but are limited to culturable and fast-growing microorganisms. As a result, studies integrating community-level dynamics with isolate-based functional validation remain limited, particularly in tropical and Indo-Pacific mangrove ecosystems (Sheng et al. 2021).

In Indonesia, despite increasing attention to plastic pollution in mangrove habitats, studies linking plastisphere microbial succession with experimentally validated LDPE degradation remain scarce. Most previous research has focused either on community profiling or on individual isolate degradation assays, without establishing direct relationships between microbial dynamics and degradation performance (Ligo et al. 2020; Zeenat et al. 2021). This limitation constrains a comprehensive understanding of the ecological mechanisms underlying plastic biodegradation in natural environments.

Therefore, this study integrates culture-independent and culture-dependent approaches to investigate LDPE biodegradation in mangrove sediments from Pamekasan, East Java. The objectives are to: (i) characterize bacterial community succession during LDPE-driven enrichment using ASV-based metagenomic analysis, (ii) identify persistent and dominant taxa associated with LDPE utilization, and (iii) evaluate the degradation potential of selected isolates using gravimetric, FTIR, and SEM-EDX analyses. We hypothesize that: (i) successive LDPE enrichment reduces community richness while increasing dominance of specialized degradative taxa; and (ii) taxa persisting across enrichment stages exhibit higher degradation efficiency than transient members. This integrative approach is expected to provide insights into the ecological basis of LDPE biodegradation in mangrove plastisphere systems and support biodiversity-based strategies for mitigating plastic pollution in coastal ecosystems.

MATERIALS AND METHODS

Sampling area

The samples used in this study were sediment soils contaminated with plastic, collected from the mangrove ecosystem in Pamekasan, East Java Province, Indonesia. Sediments were collected at a depth of roughly 2-10 cm beneath sea level. Sampling was conducted at three different stations: Tlanakan Beach (7°13'15"S 113°26'27"E), Kotasek Beach (7°13'52"S 113°33'05"E), and Talang Siring Beach (7°08'15"S 113°35'23"E) (Figure 1). These sites were selected due to the high abundance of plastic bags found in the surrounding mangrove areas and to represent the western, eastern, and central coastal regions of Pamekasan. The collected samples were placed in zip-lock bags, transported to the Biology Laboratory of Universitas Sebelas Maret (UNS), Indonesia, in an icebox, and promptly stored at -80°C for preservation.

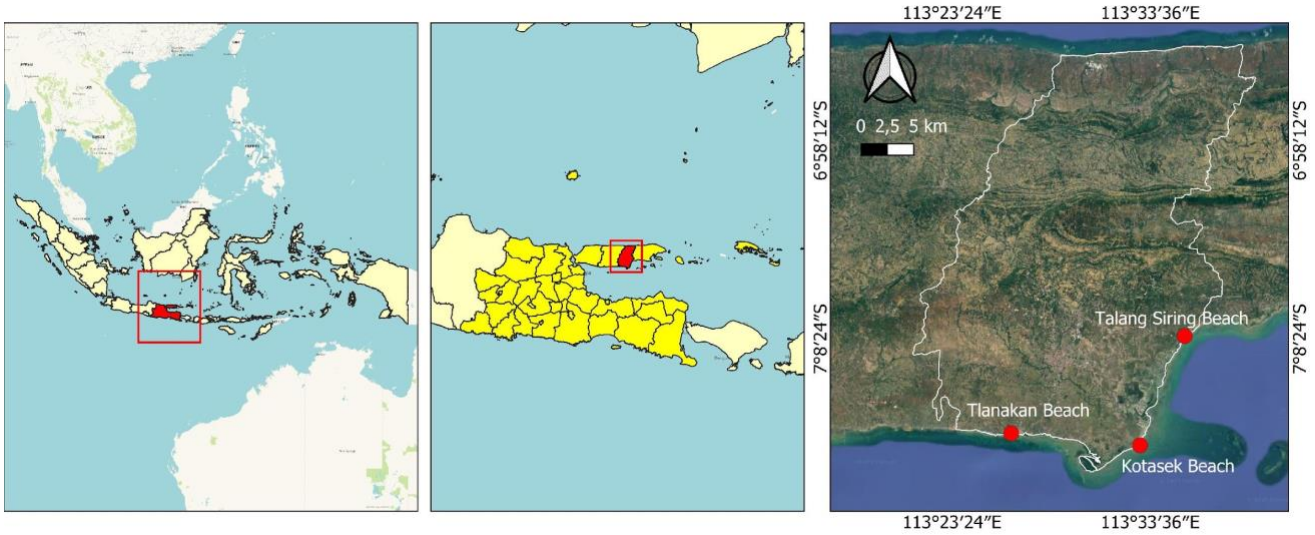

Figure 1. Sampling location of sediment in Pamekasan, East Java Province, Indonesia

Procedures

Enrichment cultures

Bacterial enrichment was conducted in three successive stages: primary, secondary, and tertiary cultures. 1 g of mangrove sediment collected from each sampling site was homogenized in 20 mL of sterile 0.85% (w/v) NaCl solution and incubated at 30°C with shaking at 180 rpm for 2-3 hours to create a composite sample for the enrichment. Subsequently, 100 µL of the homogenate was inoculated into 10 mL of modified Carbon-Free Marine (CFM) medium supplemented with LDPE beads as the sole carbon source (primary culture; Culture-1).

The modified low-carbon marine medium used in this study was prepared as per Rong et al. (2024). It consisted of (per liter of deionized water): 1 g NH_4Cl, 1 g KH_2PO_4, 1 g $K_2HPO_4 \cdot 3H_2O$, 0.2 g $MgSO_4 \cdot 7H_2O$, 20 g NaCl, 0.001 g $FeSO_4 \cdot 7H_2O$, 0.001 g $ZnSO_4 \cdot 7H_2O$, 0.001 g $MnSO_4 \cdot H_2O$, and 0.001 g $CuSO_4 \cdot 5H_2O$. A vitamin solution (0.1%, v/v) was added, containing nicotinic acid (1 g), thiamine hydrochloride (1 g), vitamin B6 (0.5 g), vitamin B12 (0.01 g), calcium pantothenate (0.5 g), and folic acid (0.5 g) per liter. The pH was adjusted to 7.0. The vitamin solution was added at low concentration to support basal metabolic activity and was not intended to serve as a primary carbon source.

Primary cultures were incubated at 30°C and 120 rpm for 30 days. Subsequently, 1 mL of Culture-1 was transferred into 100 mL of fresh CFM medium containing 0.5 g LDPE beads to establish the secondary culture (Culture-2). The tertiary culture (Culture-3) was prepared using the same procedure. All enrichment stages were performed in triplicate. Aeration was provided exclusively by orbital shaking, without additional light or pressure regulation. Linear low-density polyethylene (LLDPE) used in this study was purchased from an online marketplace (Tokopedia) as "LLDPE *murni* polyethylene PE *bubuk plastik biji plastik murni*" (*Tokopedia.com*). No formal product code from a specific manufacturer was documented by the seller; instead, the material was supplied as standard LLDPE resin suitable for plastic processing. Based on typical specifications for industrial LLDPE, the polymer has a density range of ~0.91-0.94 g/cm³, a melting point between ~120-130°C, and exhibits high tensile strength, elongation at break, and chemical resistance, consistent with general LLDPE performance used in experimental polymer studies. Culture growth was monitored by measuring optical density at 600 nm (OD600). The three-stage enrichment strategy was applied to progressively select LDPE-degrading communities, whereby primary cultures recovered native microbiota, secondary cultures reduced non-degraders, and tertiary cultures enriched specialized degradative populations.

DNA extraction

At the end of each incubation period, 2 mL of culture was collected and centrifuged at 10,000 rpm for 10 min, and the pellet was retained. DNA was extracted from the samples using the ZymoBIOMICS™ DNA Miniprep Kit following the manufacturer's protocol, and the extracted DNA was stored at -80°C. The quality and quantity of DNA were assessed using a biophotometer (Eppendorf BioPhotometer Plus), and DNA bands were visualized on 1% agarose gel electrophoresis at 85 V for 60 min.

Amplicon (16S rRNA) sequencing

DNA from triplicate cultures per enrichment stage was pooled prior to sequencing. While this approach represents the replicate cultures, it limits independent assessment of variability between biological replicates at the sequencing level. The extracted genomic DNA was submitted to a commercial sequencing facility (Genetika Science, Tangerang, Indonesia) for 16S rRNA amplicon sequencing. The V4 hypervariable region of the 16S rRNA gene was amplified using the primer pair 515F/806R (16SV4). The V4 hypervariable region of the 16S rRNA gene was amplified using the primer pair 515F/806R (16SV4), a widely adopted approach for microbial community profiling using short-read sequencing technologies (Pinto and Bhatt 2024). Library preparation followed the Illumina 16S Metagenomic Sequencing Library Preparation protocol, and paired-end sequencing was conducted on the Illumina NovaSeq platform.

Raw paired-end reads were processed using Cutadapt to remove adapter sequences and primer regions. A maximum error rate of 0.1 and a minimum read length of 200 bp were applied during trimming. Quality filtering, denoising, and chimera removal were conducted using the DADA2 pipeline, which remains a robust and reproducible approach for ASV-based microbiome analysis (Lehr et al. 2025). Taxonomic classification was performed against the SILVA 138.2 reference database (99% OTU similarity). ASVs unassigned at the phylum level or classified as chloroplast/ mitochondria were removed prior to downstream analysis. Samples were rarefied to an even sequencing depth before alpha- and beta-diversity calculations.

All ecological and statistical analyses were performed using RStudio (R version 4.2.3) with the following packages: phyloseq, vegan, microbiome, and ggplot2. Community composition was visualized using Krona Tools (https://github.com/marbl/Krona). Functional prediction of metabolic pathways was conducted using PICRUSt2 (https://github.com/picrust/picrust2) with default settings, including HMMER for hidden Markov model alignment and MinPath for pathway inference. Alpha-diversity metrics (Shannon, Simpson, and Chao1 richness) were computed using rarefied ASV tables at an equal sequencing depth to minimize sampling bias. Beta-diversity was assessed using Bray-Curtis dissimilarity. Due to pooling DNA from triplicate cultures per enrichment stage, statistical tests comparing microbial communities (e.g., PERMANOVA) could not be applied. Observed differences in community composition are descriptive rather than statistically validated.

Isolation and identification of dominant bacteria

The dominant bacterial isolates obtained from the tertiary enrichment culture were grown on Marine Agar medium following serial dilution. The cultures were incubated at 30°C for 48-72 hours. Purification was carried out by streaking individual bacterial colonies until pure isolates were obtained. The purified isolates were subsequently inoculated into Marine Broth and incubated

for 1-2 days at 30°C. The bacterial colonies grown on solid media were analyzed phenotypically by observing colony morphology and performing Gram staining, which remains a fundamental approach for preliminary bacterial characterization (Singh et al. 2025).

Genomic DNA from the selected bacterial isolates cultured in liquid media was extracted using the GeneAid Bacteria DNA Extraction Kit. DNA amplification was performed by polymerase chain reaction (PCR) using 16S rRNA primers 63F (5′-CAG GCC TAA CAC ATG CAA GTC-3′) and 1387R (5′-GGG CGG WGT GTA CAA GGC-3′) for 35 cycles. The PCR products were visualized by electrophoresis on a 1% agarose gel. Subsequently, the amplified products were sent to Genetika Science (Indonesia) for sequencing using the Sanger sequencing method, which is still widely used for accurate taxonomic identification of pure isolates (Rodriguez-Pazmiño et al. 2025). The resulting chromatograms were edited using BioEdit, and sequence identification was conducted through BLAST analysis on the NCBI (National Center for Biotechnology Information) database. The 16S rRNA gene sequences generated in this study have been deposited in the NCBI GenBank database under accession numbers PX980572-PX980579.

Degradation analysis of LDPE plastics

Low-Density Polyethylene (LDPE) sheet used in this study was obtained from an online marketplace (Tokopedia). The product was supplied as a clear LDPE plastic sheet with an approximate thickness range of 0.05-0.50 mm; no formal manufacturer's product code or certified datasheet was provided by the seller. LDPE plastic sheets (1 × 1 cm²) were weighed to determine their initial mass and observed under a Scanning Electron Microscope (SEM) for surface characterization. The plastics were then introduced into Bushnell Haas (BH) medium. The Bushnell-Haas medium used for the degradation analysis consisted of the following components: 1.0 g/L ammonium nitrate (NH_4NO_3), 0.2 g/L magnesium sulfate heptahydrate ($MgSO_4 \cdot 7H_2O$), 1.0 g/L dipotassium phosphate (K_2HPO_4), 0.1 g/L calcium chloride dihydrate ($CaCl_2 \cdot 2H_2O$), and 0.15 g/L potassium chloride (KCl) (Montazer et al. 2020). Each bacterial isolate was inoculated into the medium at a concentration of 10% (v/v), while the control was prepared without bacterial inoculation. The cultures were incubated at room temperature with shaking at 120 rpm for 30 days. To ensure reliable degradation measurements, LDPE films (1 × 1 cm²) were sterilized by autoclaving, weighed, and examined by SEM before use. All treatments were conducted in triplicate with an uninoculated medium as a control. At each 10-day interval, LDPE pieces were cleaned in 70% ethanol for 30 min, rinsed with distilled water, dried at 60°C for 1 h, and reweighed to avoid residue-related weight artifacts. The percentage of weight loss was calculated using the following formula:

$$\text{Weight loss (\%)} = \frac{W0 - Wt}{W0} \times 100\%$$

Where:
W0 : initial weight (g)
Wt : final weight (g)

At the end of the incubation period, the surface morphology of the LDPE samples was analyzed using Scanning Electron Microscopy (SEM) equipped with Energy Dispersive X-ray (EDX) detectors. In addition, Fourier Transform Infrared Spectroscopy (FTIR) analysis was performed to identify structural changes and the formation of new functional groups in the LDPE polymer matrix. Carbonyl and hydroxyl indices were calculated as the ratio of absorbance at ~1650-1700 cm^{-1} and 3200-3600 cm^{-1} to the reference band at ~1460 cm^{-1}. Due to the absence of replicate FTIR measurements, statistical comparison of CI and HI values was not feasible. Prior to FTIR, LDPE films were rinsed with 0.85% NaCl, washed three times with distilled water, gently sonicated to remove biofilm without damaging the polymer, and dried in a desiccator or at 35-45°C. For SEM, samples were rinsed with 0.85% NaCl, fixed in 4% formaldehyde, washed with PBS, and dehydrated through an ethanol series before final drying. These procedures minimized sample distortion and ensured that observed changes were due to microbial activity rather than handling effects. SEM images were analyzed using ImageJ web-based software. Images were calibrated using scale bars and converted to 8-bit grayscale. Surface damage parameters, including crack area percentage, pore density, average pit diameter, and 2D roughness index, were quantified using thresholding and particle analysis.

Data analysis

Metagenomic data were analyzed using bioinformatics tools such as Krona, PICRUSt2, and R Studio. Bacterial sequence data were contig-assembled and cleaned to remove background noise using BioEdit, and sequence similarity was determined by performing BLAST analysis against the NCBI database. Statistical tests were done for cell density and LDPE weight-loss (%). Data were tested for normality using the Shapiro-Wilk test and for homogeneity of variance using Levene's test. For cell density (CFU mL^{-1}) and LDPE weight-loss (%) measurements, one-way ANOVA followed by Tukey's honest significant difference (HSD) test was applied when both assumptions were met. Qualitative data on changes in functional groups of LDPE after the degradation test were analyzed using Fourier Transform Infrared Spectroscopy (FTIR). The FTIR spectra were interpreted by examining the characteristic peaks and band patterns corresponding to specific functional groups, indicating structural modifications of the polymer matrix.

RESULTS AND DISCUSSION

Bacterial growth profile during three-stage enrichment on LDPE

The first stage of the experiment involved enrichment culture, which produced three sequential culture samples: primary, secondary, and tertiary cultures. The optical density at 600 nm (OD_{600}) was measured to assess bacterial growth in each culture following a 30-day incubation period. The highest average OD_{600} values was 0.2157±0.016 for the

primary culture, and the lowest was 0.2003±0.012 for the tertiary culture (Figure 2). This reduction indicates there are selection phenomena towards the bacterial growth in each culture. Based on the results of one-way ANOVA, no significant differences in cell density were observed among the three enrichment cultures ($p = 0.732 > 0.05$). This may be because the enrichment cultures did not drastically reduce the total number of cells, but instead promoted changes in community composition and bacterial dominance.

16S rRNA amplicon sequencing analysis

Alpha diversity

The alpha diversity index (Table 1) serves as a metric for characterizing the average species diversity within a specific location or habitat on a local scale. The highest richness values were obtained in the primary culture, followed by the secondary and tertiary cultures, as indicated by the observed, Chao1, ACE, and Fisher indices. The Shannon and Simpson indices, on the other hand, showed a different pattern. The secondary culture had the most diversity, followed by the tertiary and primary cultures. The Shannon index reached its highest value in the secondary culture (3.74), while the Simpson index was closest to 1 (0.969), indicating a more balanced community with a more even distribution of species abundance. Based on Observed, Chao1, and ACE results, there is a decrease in amplicon sequence variants (ASVs) throughout the enrichment process. The primary culture exhibited the highest ASV richness with 134 ASV, followed by 82 ASVs in the secondary culture and 67 ASVs in the tertiary culture.

The rarefaction curves of all samples tended to approach a plateau, indicating that the sequencing depth was sufficient to capture the majority of bacterial diversity within each sample (Figure 3). The asymptotic nature of the curves suggests that additional sequencing would yield only a limited number of new ASVs, confirming that the obtained sequencing coverage was adequate for downstream diversity analyses.

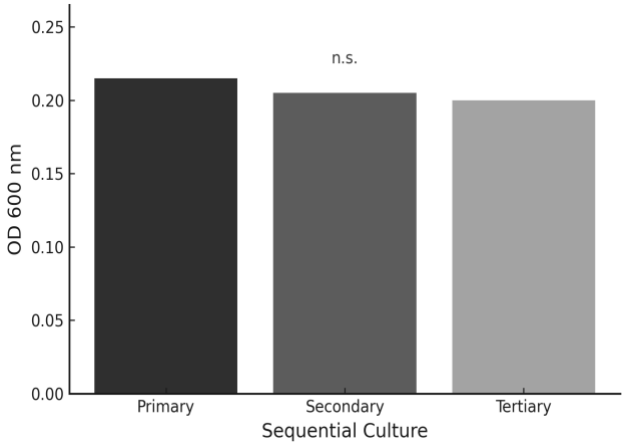

Figure 2. The optical density of the end sequential culture (primary, secondary, and tertiary). Note: Primary (the first culture taken directly from the sample), Secondary (subculture from the primary stage), Tertiary (subculture from the secondary stage). No significant differences were observed among cultures (one-way ANOVA, $p>0.05$). Error bars represent standard deviation (n = 3)

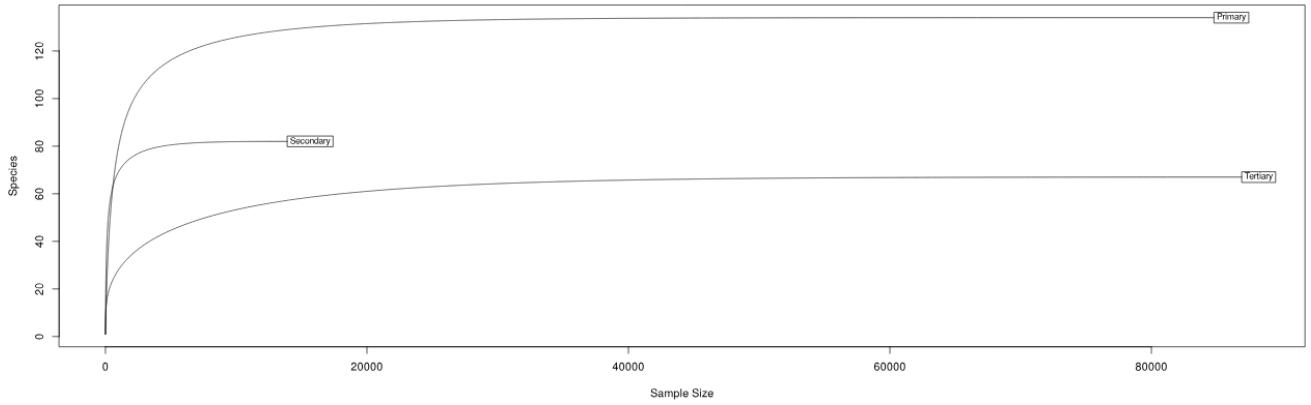

Figure 3. Rarefaction curves of ASVs sampling depth

Table 1. Alpha diversity index

Culture stage	Observed	Chao1	ACE	Shannon (H')	Simpson (D)	Fisher
Primary	134	134	134	1.86	0.533	15.55
Secondary	82	82	82	3.74	0.969	11.34
Tertiary	67	67	67	2.46	0.888	7.11

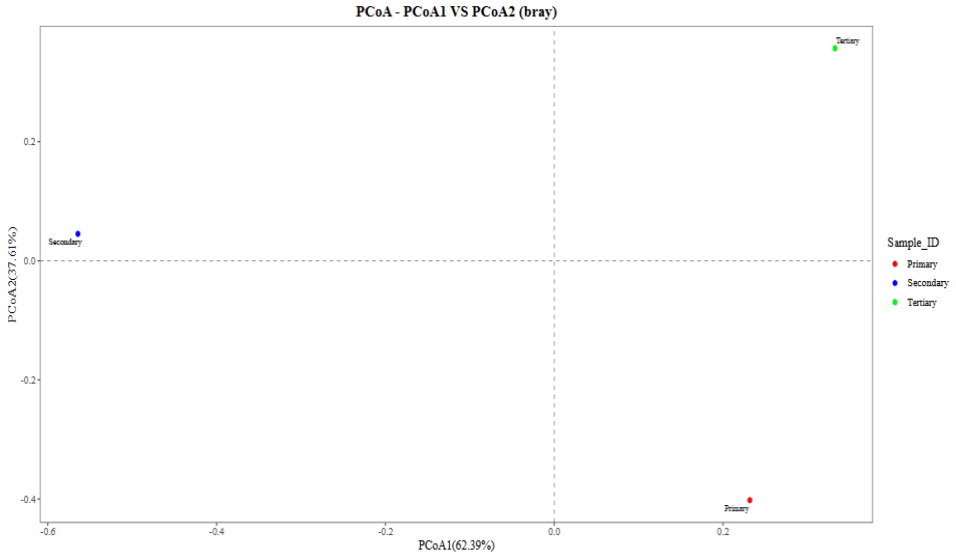

Figure 4. Beta diversity of different culture stages (Primary, Secondary, and Tertiary)

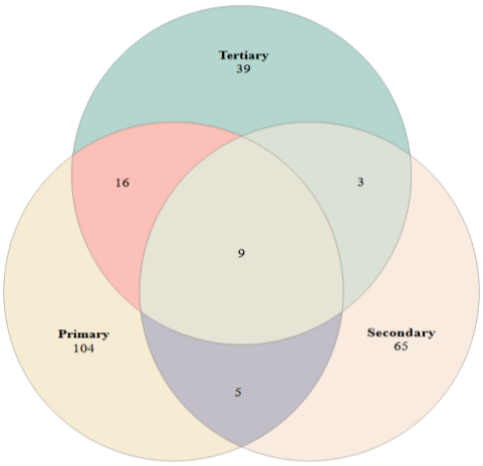

Figure 5. Venn diagram of microbial communities at ASVs level among primary, secondary, and tertiary cultures

Beta diversity

A beta diversity analysis of the microbial community was conducted (Figure 3). A principal coordinates analysis (PCoA) with the Bray-Curtis matrix was performed to decompose the sample distance matrix and display the natural distribution of samples at a specific distance scale. The primary culture (red dot) was located at the lower right, the secondary culture (blue dot) at the left, and the tertiary culture (green dot) at the upper right. The contribution rates of axes 1 and 2 were 62.39% and 37.61%, respectively. PCoA1 represents the main influence of the selection process during the enrichment culture. Therefore, the higher the percentage of PCoA1, the greater the difference in community composition between stages. PCoA2 represents secondary differences following PCoA1, such as adaptation to the LDPE substrate or the dominance of certain bacterial groups. The observed separation along PCoA1 suggests that the enrichment process selectively favored microbial taxa capable of utilizing LDPE as a carbon source, leading to significant compositional shifts from the primary to tertiary cultures. The distinct positions along PCoA2 indicate secondary ecological processes, such as competition, substrate specialization, or the establishment of dominant degraders within each stage.

Venn diagrams serve as valuable tools for comparing species diversity or groups of organisms across different environmental conditions (Figure 5). The three enrichment cultures shared nine ASVs, indicating that these nine ASVs represent bacterial communities capable of adapting and potentially utilizing LDPE as their substrate. The primary culture shared five ASVs with the secondary culture and 16 ASVs with the tertiary culture, while the secondary and tertiary cultures shared three ASVs. There are 39 unique ASVs found only in tertiary culture (Figure 4).

Taxonomic profiles of bacterial communities in sample cultures

According to the ASVs clustering results, species information and species-based abundance distribution for the three samples were obtained. Figure 6 depicts species abundance detected at different taxonomic levels. In total, 16 identified phyla were observed, and ten phyla were identified at an abundance >1%. At the phylum level, Pseudomonadota (89.17%), Bacteroidota (3.61%), and Bacillota (2.32%) were dominant in primary cultures. In secondary cultures, Pseudomonadota (33.27%), Bacillota (24.95%), and Actinomycetota (12.98%) were the most abundant phyla. In tertiary cultures, Pseudomonodota (71.46%), Bacteroidota (26.32%), and Dadabacteria (1.85%) were dominant. When the ASVs were considered at the genus level, a high diversity of microbes was identified. In primary and secondary cultures, the largest genera were *Acinetobacter* (68.3%) and *Staphylococcus* (9.57%). In tertiary culture, the three most dominant genera were *Qipengyuania* (20.76%), *Flavobacterium* (17.08%), and *Pseudoxanthomonas* (11.46%) (Figure 6.B). The top 10 dominant genera were *Acinetobacter*, *Qipengyuania*, *Pseudomonas*, *Caulobacter*, *CSP1-2*, *Sphingopyxis*, *Paramesorhizobium*, *Methylorubrum*, *Brevundimonas*, and *Methylobacterium*.

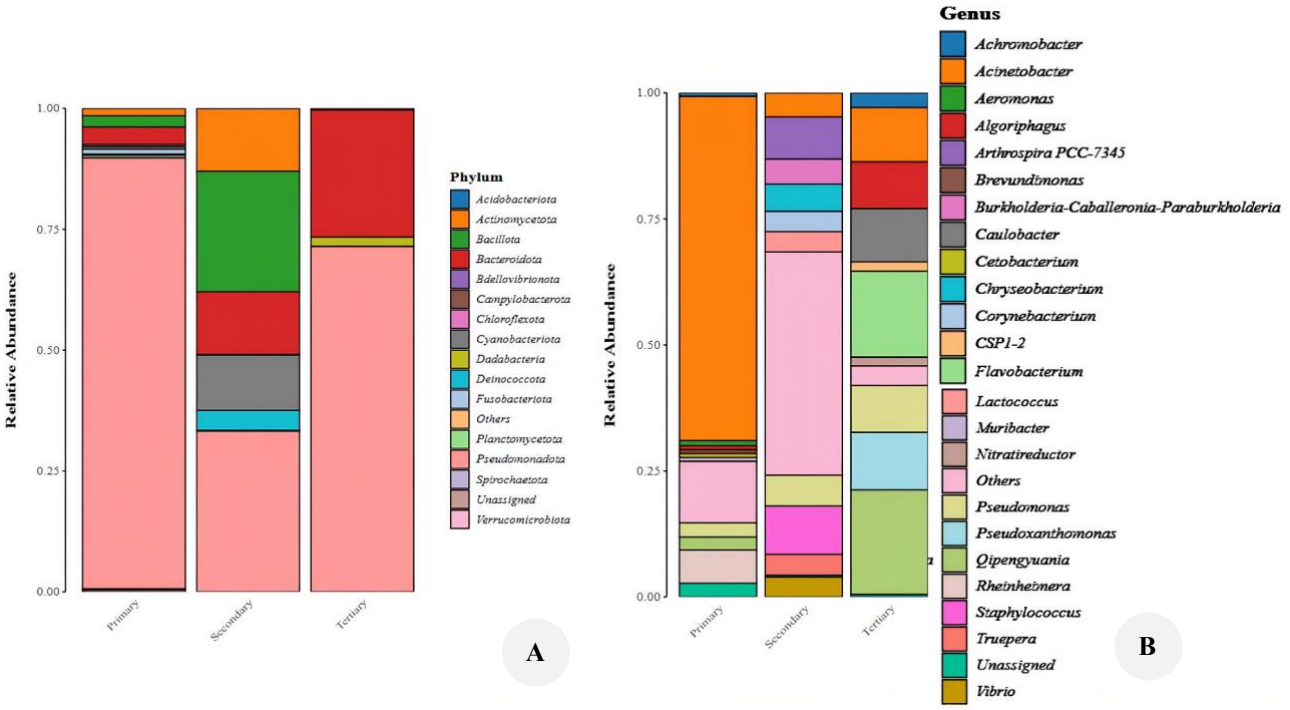

Figure 6. Relative abundances of the dominant bacteria in each sample. A. Phylum, B. Genus

Identification of selected bacteria

In this study, bacterial isolation was performed following the tertiary enrichment stage to recover cultivable microorganisms with potential LDPE-degrading activity. Although amplicon sequencing revealed several dominant taxa in the enriched communities, the isolation procedure primarily targeted viable and fast-growing bacteria capable of forming colonies under laboratory conditions. As a result, the recovered isolates represent the cultivable fraction of the LDPE-enriched consortia rather than the most abundant taxa detected by sequencing analysis.

A total of eight bacterial isolates (Isolates 1-8) were obtained from the tertiary culture (Table 2). Preliminary phenotypic characterization was conducted using Gram staining and microscopic observation at 400× magnification. The analysis showed that three isolates were Gram-positive and five were Gram-negative, with all isolates exhibiting rod-shaped (bacillus-like) morphology.

The molecular identification process was carried out through the amplification of the 16S rRNA gene using a universal primer pair, 63F (5′-CAG GCC TAA CAC ATG CAA GTC-3′) and 16S rRNA_1387R (5′-GGG CGG WGT GTA CAA GGC-3′). The amplification results visualized on agarose gel electrophoresis showed a clear single DNA band at approximately 1,500 bp, corresponding to the expected fragment size of the bacterial 16S rRNA gene. The 16S rRNA gene sequencing results were analyzed using the BLASTn (Basic Local Alignment Search Tool) program available in the NCBI database to determine the level of similarity between the nucleotide sequences of the isolates and those of previously identified bacterial species. The percentage of sequence similarity between the isolates and reference strains ranged from 97-100%, indicating a close genetic relationship with species registered in the database. A similarity value of ≥99% is generally considered the threshold for species-level similarity (Waymire et al. 2024). Based on the BLAST analysis, the obtained isolates exhibited high similarity to several bacterial species previously reported to have potential roles in plastic degradation, as shown in Table 3. The 16S rRNA gene sequences generated in this study have been submitted to the NCBI GenBank database and are currently under review. Accession numbers will be provided upon acceptance.

Table 2. Characterization of bacterial isolates from tertiary cultures

Code of isolates	Gram	Morphology
K1	Positive	Rod
K2	Negative	Rod
K3	Negative	Rod
K4	Negative	Rod
K5	Positive	Rod
K6	Negative	Rod
K7	Positive	Rod
K8	Negative	Rod

Table 3. Molecular identification results of bacterial isolates

Code of isolates	Fragment length (bp)	BLAST similarity (%)	Closest relative (NCBI)	Accession number
K1	1457	100	*Brevibacterium oceani*	MH917919.1
K2	1426	99.88	*Microbacterium aurantiacum*	AB610602.1
K3	1438	100	*Microbacterium* sp.	AB847928.1
K4	1408	100	*Aeromonas veronii*	OL885242.1
K5	1470	99.68	*Bacillus* sp.	ON571736.1
K6	1431	99.79	*Brucella daejeonensis*	MN258541.1
K7	1351	92.08	Uncultured Nocardiaceae	KY271068.1
K8	1476	100	*Aeromonas jandaei*	KF908778.1

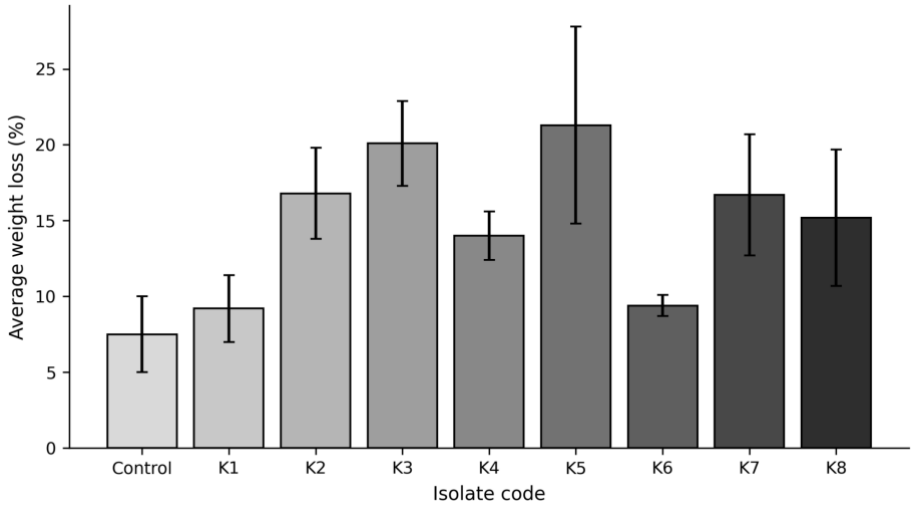

Figure 7. Average plastic weight loss during 30 days incubation

Percentage of plastic weight reduction

The LDPE plastic samples exposed to several bacterial isolates showed variations in apparent mass loss after 30 days of incubation (one-way ANOVA, $p = 0.001 < 0.05$). The highest average apparent mass loss was observed in LDPE treated with *Bacillus* sp. K5 (21.35%), followed by *Microbacterium* sp. K3 (20.27%), and *Microbacterium aurantiacum* K2 (17.10%). Control samples without bacterial inoculum also exhibited a reduction in mass (7.75%), indicating that part of the observed apparent mass loss may be attributed to additive leaching or handling artefacts rather than microbial activity alone. These data are presented as preliminary indicators of substrate-associated microbial activity rather than definitive evidence of LDPE biodegradation (Figure 7).

Analysis of FTIR results

After conducting the plastic weight reduction analysis as an initial indicator of degradation, the next step was to examine the changes in functional groups on the LDPE surface using Fourier Transform Infrared Spectroscopy (FTIR) was performed to identify chemical modifications occurring in the polymer structure as a result of microbial activity during the degradation process. Figure 8 presents the FTIR spectra obtained from the control, *M. aurantiacum* K2, *Microbacterium* sp. K3, and *Bacillus* sp. K5 samples, showing the wavelength positions of the peaks generated in the FTIR analysis. These peaks allow for the prediction of polymer structural changes, which may indicate modifications occurring during the degradation test. To clarify the differences among the spectra, a more detailed presentation of the peak values is provided in Table 4.

The FTIR spectra revealed clear shifts from the untreated LDPE baseline, where no oxidative bands were present, indicating pristine LDPE polymer. Incubation with *M. aurantiacum* K2 resulted in the appearance of carbonyl bands and changes in C-H intensities, reflecting early oxidative modification and initial depolymerization of the LDPE surface. *Microbacterium* sp. K3 induced hydroxyl and carbonyl/amide-associated signals, indicating a degradation mechanism involving both oxidative transformation and biofilm-mediated surface interaction. The clearest changes were observed in the *Bacillus* sp. K5 treatment, which exhibited strong OH and carbonyl peaks and marked alterations in C-H bands, indicating intensive surface oxidation and chain scission. Collectively, these patterns demonstrate progressive oxidative degradation across isolates, with *Bacillus* sp. K5 shows the highest efficiency in modifying and breaking down the LDPE structure. Table 5 shows the key FTIR peaks changes.

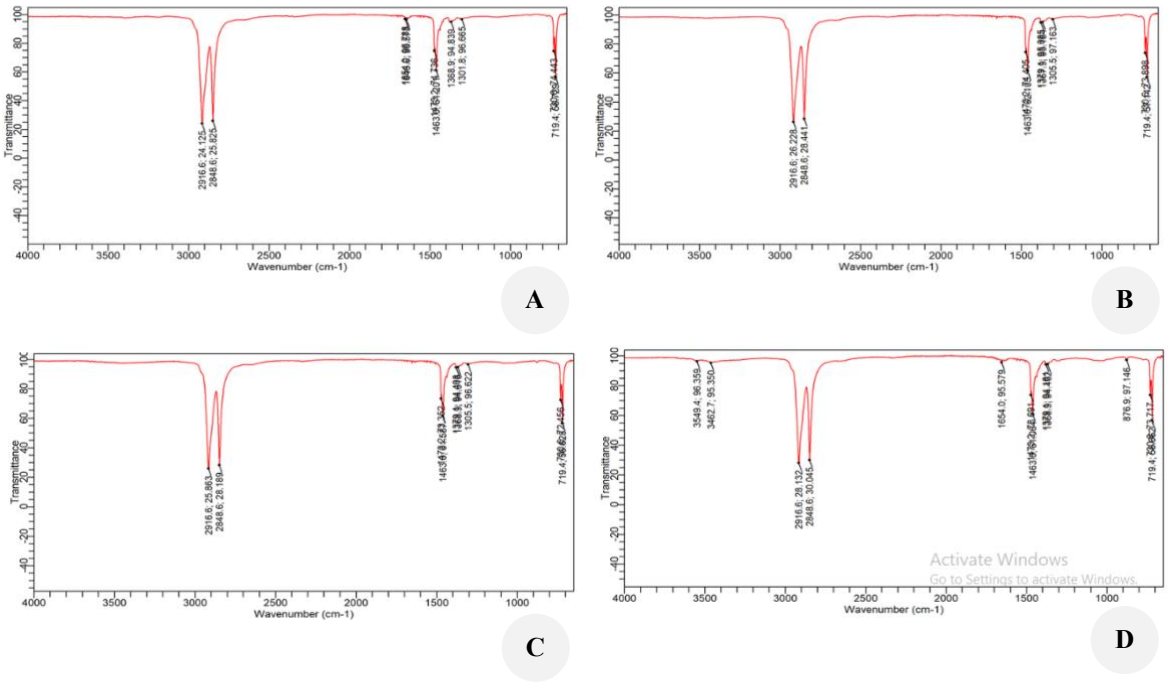

Figure 8. FTIR spectra of plastic after degradation test. A. Control, B. *Microbacterium aurantiacum*, C. *Microbacterium* sp., and D. *Bacillus* sp.

Table 4. Peak spectrum values in FTIR results

Wavenumber (cm^{-1})	Intensity	Possible functional groups	General interpretation	Sampel
719.37-730.56	56.66-73.72	CH_2 rocking	Characteristics of the LDPE main chain	Control, K2, K3, K5
1301.77-1368.86	94.84-96.66	CH_2/CH_3 wagging - twisting	Sign of a saturated hydrocarbon chain	Control, K2, K3, K5
1462.98-1473.23	61.20-74.74	CH_2 scissoring	Long methylene chains	Control. K2, K3, K5
1646.55-1654	96.57-96.79	C=C stretching / amide I	Presence of double bonds or residual water/protein	Control
2848.62-2916.64	24.12-25.82	Stretching C-H from -CH_2-	Aliphatic (C-H) bonds	Control, K2, K3, K5
1305.50-1379.12	95.08-97.16	CH_2/CH_3 wagging-twisting	Slight change from control	K2 and K3
1368.87-1379.12	94.16-94.46	CH_2/CH_3 wagging-twisting	LDPE crystallinity decreased	K5
1654.01	95.58	Conjugated C=O / Stretching C=C	Sign of advanced polyethylene oxidation	K5
3462.70-3549.36	95.35-96.36	-OH (hydroxyl) group /N-H (amide)	Advanced LDPE oxidation or biofilm residue	K5

Table 5. Key peaks changes

Treatment	Peak (cm^{-1})	Type of change	Interpretation
Microbacterium aurantiacum K2	1305-1379	Appearance / shift	CH_2/CH_3 wagging-twisting → slight modification of hydrocarbon chains
	2848-2916	Intensity change	Minor reduction in C-H stretch → early chain modification
Microbacterium sp. K3	1305-1379	Appearance / shift	CH_2/CH_3 wagging-twisting → change in hydrocarbon chain structure
	2848-2916	Intensity change	Reduction in C-H stretch → polymer chain disturbance
Bacillus sp. K5	1368-1379	Appearance / shift	Decreased LDPE crystallinity → structural rearrangement
	1654	Appearance	Conjugated C=O / C=C → advanced oxidation
	3462-3549	Appearance	-OH / N-H → surface hydroxylation or biofilm residue
	2848-2916	Intensity change	C-H reduction → chain scission

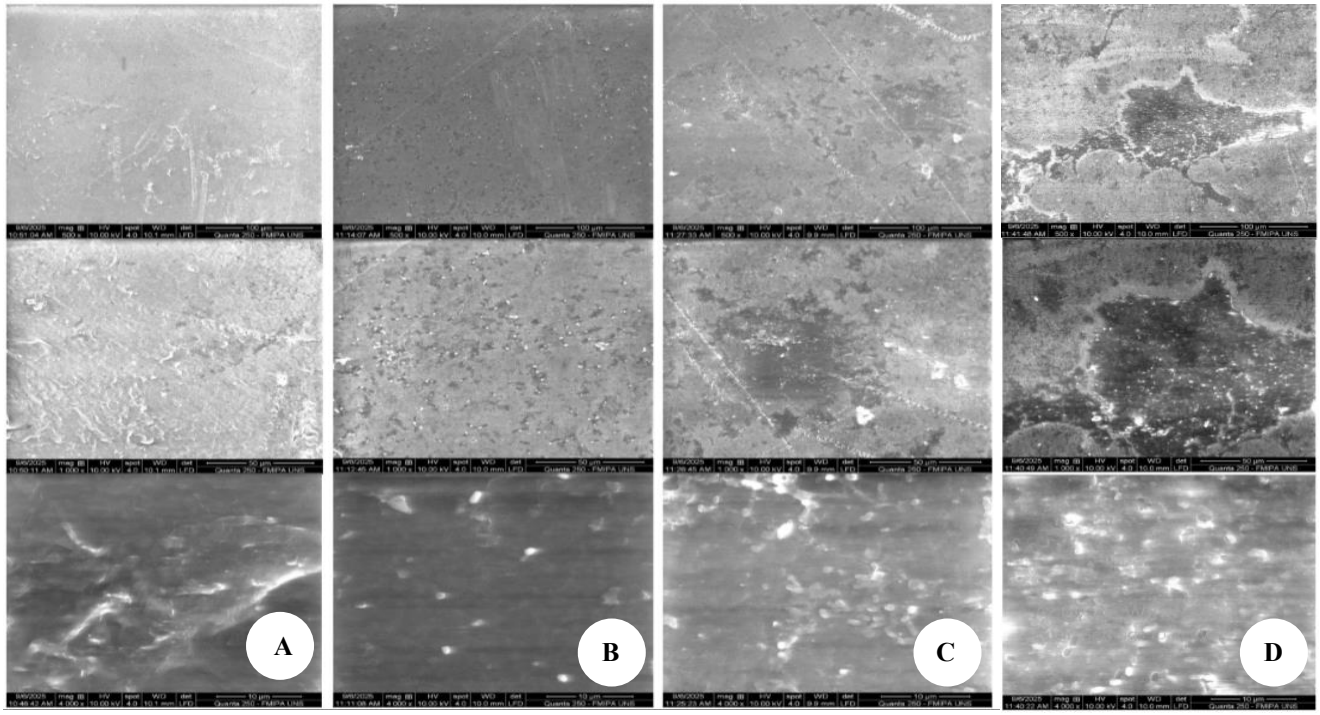

Figure 9. SEM analysis of tested plastic. A. Control, B. *Microbacterium aurantiacum*, C. *Microbacterium* sp., and D. *Bacillus* sp.

Table 6. Carbonyl and hydroxyl indices of LDPE samples

Sample	A1460 (Ref)	A(C=O)*	A(OH)**	CI	HI
Control	61.20	ND	ND	~0	~0
K2	61.20	ND	ND	~0	~0
K3	61.59	ND	ND	~0	~0
K5	61.06	95.58 (1654 cm^{-1})	95.85 (3462-3549 cm^{-1})	1.57	1.57

Note: A1460: reference band (CH_2 bending), A(C=O): absorbance at 1650-1700 cm^{-1}, A(OH): average absorbance at 3200-3600 cm^{-1}, ND: Not detected, *: Carbonyl-related band, **: Hydroxyl stretching band

Table 6 shows the carbonyl index (CI) and hydroxyl index (HI) values of the LDPE samples. The control, K2, and K3 samples showed no distinct carbonyl (1700-1740 cm^{-1}) or hydroxyl (3200-3600 cm^{-1}) bands, resulting in negligible CI and HI values. In contrast, sample K5 exhibited weak absorption bands at ~1654 cm^{-1} and 3462-3549 cm^{-1}, corresponding to carbonyl- and hydroxyl-related functional groups, with CI and HI values of 1.57. These results indicate initial oxidative modification of LDPE under the experimental conditions.

Analysis of SEM results

The surface morphology of LDPE samples was examined using Scanning Electron Microscopy (SEM) to observe structural changes following incubation with bacterial isolates. This analysis was conducted to compare surface features between control and treated samples. Differences in surface topography, including the presence of cracks, grooves, pits, and surface irregularities, were observed in the treated samples compared to the control. The SEM micrographs of the analyzed samples are presented in Figure 9.

To further characterize surface modifications, Energy Dispersive X-ray Spectroscopy (EDS) was performed to analyze the elemental composition of the LDPE surface. The EDS analysis focused on the relative abundance of carbon (C), oxygen (O), and other detected elements. Variations in elemental composition among the samples are presented in Figure 10. These results provide complementary information to the SEM observations by describing changes in surface elemental profiles following bacterial treatment.

Quantitative analysis of SEM images was performed to evaluate surface morphological parameters of LDPE samples, including crack area, pore density, average pit diameter, and two-dimensional surface roughness at magnifications of 100, 50, and 10 µm (Table 7). The control samples showed crack area values of 2.99-8.22%, pore density of 1.92×10^6-1.98×10^7 mm^{-2}, average pit diameters of 0.84-1.74 µm, and surface roughness of 43.40-70.06. K2-treated samples exhibited crack area values of 1.62-13.32%, pore density of 1.44×10^6-1.90×10^6 mm^{-2}, pit diameters of 0.60-0.76 µm, and roughness values of 32.17-86.65. For K3-treated samples, crack area ranged from 8.05% to 14.97%, pore density from 2.25×10^3 to 1.34×10^6 mm^{-2}, average pit diameter from 0.40 to 0.74 µm, and surface roughness from 69.36 to 90.97. K5-treated samples showed crack area values of 15.65-20.69%, pore density of 6.32×10^5-1.54×10^6 mm^{-2}, pit diameters of 0.67-2.30 µm, and roughness values of 92.64-103.29.

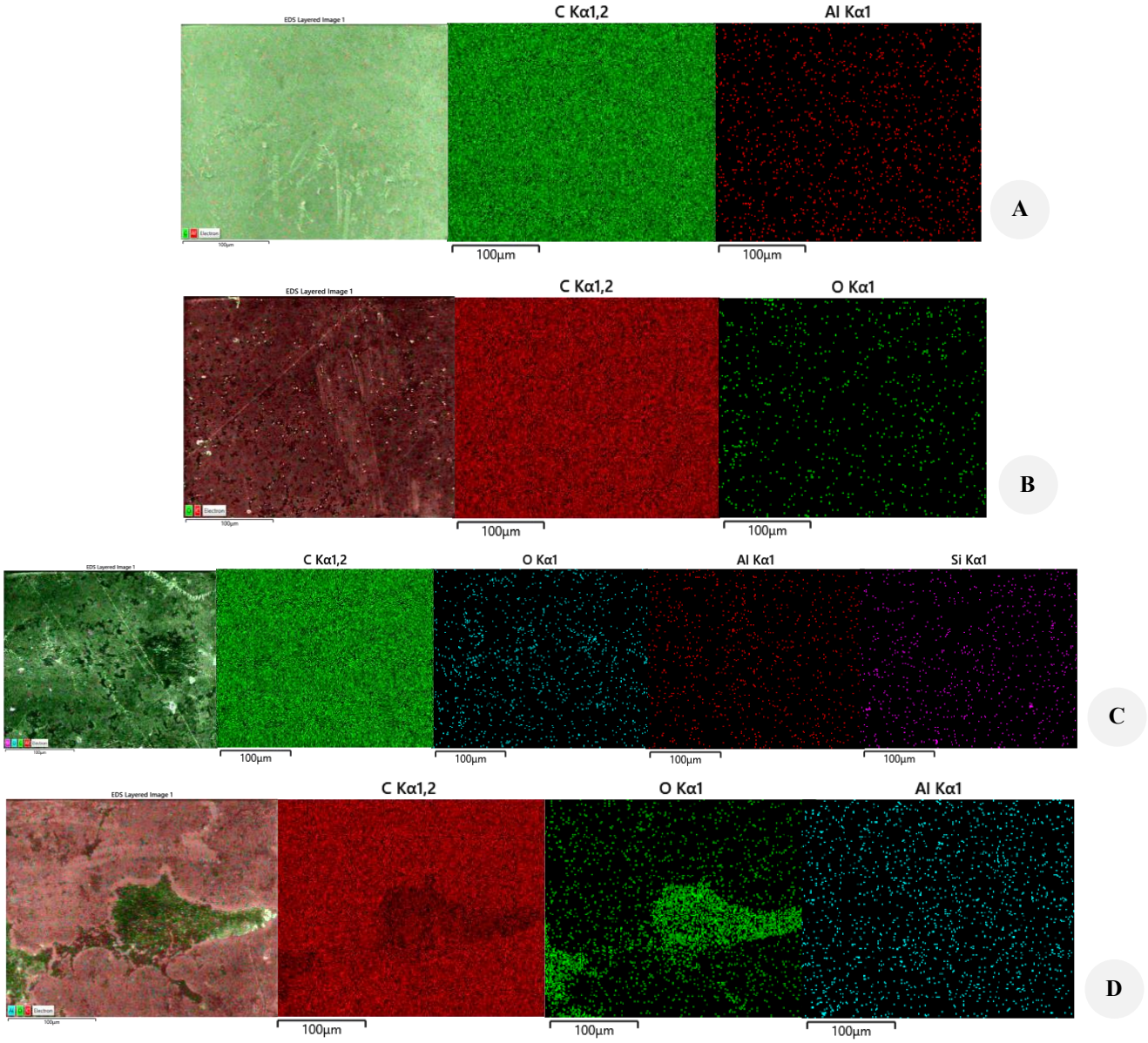

Figure 10. EDS results of test plastic (A. Control; B. *Microbacterium aurantiacum*, C. *Microbacterium* sp., and D. *Bacillus* sp.)

Table 7. Quantitative SEM surface parameters of LDPE samples analyzed by ImageJ

Sample	Mag (µm)	Crack area (%)	Pore density (mm²)	Average Pit (µm)	Roughness (2D)
Control	100	5.960	19829492	1.176	60.371
Control	50	8.224	6483295	0.839	70.058
Control	10	2.985	1915169	1.743	43.396
K2	100	5.907	1634683	0.610	60.119
K2	50	13.322	1902678	0.600	86.652
K2	10	1.618	1437076	0.761	32.170
K3	100	13.524	1090414	0.707	87.204
K3	50	14.965	1342138	0.399	90.967
K3	10	8.046	2246	0.741	69.360
K5	100	15.882	1536970	0.708	93.206
K5	50	15.647	1209743	0.674	92.641
K5	10	20.687	631591	2.300	103.290

Discussion

In this study, the enrichment process produced clear shifts in bacterial cell density and microbial composition across the three culture stages. The slight decrease in OD_{600} values from primary to tertiary culture indicates progressive selection for bacteria capable of growing on LDPE as the sole carbon source. In this study, the non-significant differences in cell density indicate that the enrichment cultures did not drastically reduce the total number of cells, but instead promoted shifts in community composition and bacterial dominance. The absence of statistically significant differences in cell density supports the interpretation that enrichment acted primarily through taxonomic replacement and dominance shifts, rather than through extensive cell lysis or toxicity-driven mortality. This pattern is consistent with previous reports showing declining biomass during serial enrichment with methane or Cs^+ ions (Kato et al. 2016; Goraj et al. 2023). Given that LDPE is chemically inert and non-toxic, the observed trends are best explained by strong selective pressure associated with its high molecular weight, hydrophobicity, and resistance to enzymatic attack, rather than starvation-induced cell death (Kimber et al. 2023). Similar enrichment-driven selection toward specialist degraders has been widely reported in studies targeting plastic- and hydrocarbon-degrading microorganisms (Rong et al. 2024; Zhang et al. 2024), underscoring the ecological consistency of the observed response.

Amplicon-based community profiling revealed pronounced microbial restructuring during the enrichment process. Alpha diversity analysis showed that species richness was highest in the primary culture, reflecting the heterogeneous composition of the original mangrove sediment. Richness progressively declined toward the tertiary stage, as indicated by decreasing Observed, Chao1, ACE, and ASV values. In contrast, the secondary culture exhibited the highest Shannon and Simpson indices, suggesting increased community evenness and diversity at this intermediate stage. The tertiary culture, which retained only 39 ASVs, represents a niche-adapted assemblage dominated by specialized LDPE degraders and associated cross-feeders (Pawano et al. 2024). This pattern is consistent with previous studies demonstrating that stepwise enrichment reduces overall richness while promoting functional specialization (Skariyachan et al. 2021). The marked decline in ASV richness from primary to tertiary cultures indicates strong substrate-driven selection, favoring taxa capable of utilizing or benefiting from LDPE-derived compounds. The elevated diversity and evenness observed in the secondary culture likely reflect an intermediate successional phase characterized by the coexistence of multiple interacting species, potentially involving cross-feeding or synergistic degradation pathways. In contrast, the reduced diversity in the tertiary culture suggests competitive exclusion and dominance by highly efficient degraders.

Beta diversity analysis based on Bray-Curtis dissimilarity revealed clear separation among enrichment stages, confirming substantial shifts in community composition during successive enrichment. Together, the declining alpha diversity and increasing inter-stage dissimilarity highlight the strong selective pressure imposed by LDPE, which progressively eliminates non-utilizing taxa and promotes the establishment of specialized microbial consortia.

ASV-based Venn analysis reinforced this interpretation. The primary culture exhibited the highest ASV richness, reflecting generalist and non-degrading taxa from mangrove sediments. Selective pressure in the secondary culture retained only LDPE-adapted taxa, whereas the tertiary culture harbored 39 unique ASVs, likely activated or enriched under specialized LDPE-driven conditions, consistent with observations in PP-enriched systems (Salinas et al. 2023; Pawano et al. 2024). Nine ASVs persisted across all stages, constituting a stable core plastisphere microbiome (Agostini et al. 2021). Transitional dynamics were evident: five ASVs shared between primary and secondary cultures represent early colonizers subsequently outcompeted, whereas three ASVs shared between secondary and tertiary cultures likely emerged in response to metabolites such as organic acids, H_2, and formate, which create new ecological niches for initially rare taxa. Sixteen ASVs shared between primary and tertiary cultures exhibited a disappearance-reappearance pattern indicative of metabolic cross-feeding, wherein "receiver" taxa depend on metabolites from "provider" taxa (Jiao et al. 2016; Dang et al. 2023). Collectively, these findings demonstrate that LDPE-driven enrichment reshapes microbial communities through the interplay of core persistence, transient colonization, and selective activation of rare taxa.

The observed taxonomic succession reflects the selective establishment of an LDPE-adapted microbial community, in which functional specialization gradually supersedes taxonomic diversity. The dominance of Pseudomonadota, particularly Gammaproteobacteria, is consistent with their well-documented capacity for polymer degradation in plastisphere environments (Bocci et al. 2024; Muangchinda and Pinyakong 2024). Concurrent increases in Bacteroidota and Actinomycetota indicate adaptive restructuring, whereby early colonizers likely initiate polymer oxidation, enabling secondary taxa to exploit oxidized metabolites and demonstrating metabolic complementarity and division of labor (Wicaksono et al. 2022).

At the genus level, *Acinetobacter*, *Pseudomonas*, and *Pseudoxanthomonas* exemplify the oxidative and hydrolytic versatility required for LDPE breakdown, while Qipengyuania and Flavobacterium likely contribute through hydrocarbon metabolism and biofilm-mediated polymer utilization. These patterns underscore the ecological relevance of multispecies interactions in shaping plastisphere communities and highlight the potential for designing synthetic consortia or enzyme-assisted bioreactors informed by amplicon-based community profiling.

Notably, the cultured isolates did not fully correspond to the dominant taxa identified through 16S rRNA amplicon sequencing. This discrepancy reflects well-documented cultivation bias, in which many abundant environmental microorganisms exhibit slow growth, specific nutrient requirements, or dependencies on interspecies interactions

that are difficult to replicate under laboratory conditions (Wang et al. 2020). Standard isolation methods tend to favor fast-growing and stress-tolerant microorganisms, whereas amplicon sequencing provides a broader, albeit incomplete, representation of community diversity. A similar pattern has been reported in study of marine sponge microbiomes, where culture-based and sequencing-based analyses often produce contrasting community profiles. In these systems, dominant taxa detected by high-throughput sequencing are frequently absent from culture collections, while many isolated strains represent only a small fraction of the total community (Hardoim et al. 2014). Consequently, the isolates obtained in this study represent the cultivable fraction of the LDPE-enriched consortia rather than the most abundant in situ taxa.

Despite this limitation, isolate analysis highlights the pivotal role of Actinobacteriota in advanced polymer degradation, while the persistence of Aeromonas and other Gammaproteobacteria suggests community resilience and functional redundancy under prolonged LDPE selection (Muangchinda et al. 2024). The survival of *Bacillus* spp. further illustrates adaptation to nutrient-limited, polymer-rich environments through endospore formation and metabolic versatility (Waqas et al. 2021). In addition, the detection of *Brucella daejeonensis* extends the ecological range of certain Brucella species to plastisphere-associated biofilms, suggesting potentially overlooked contributions to polymer-associated microbial networks (Muthukumar et al. 2003; Zettler et al. 2013).

Collectively, these findings indicate a transition from diverse initial assemblages to a streamlined, functionally optimized consortium driven by strong substrate-mediated selection. Although cultivation bias limits direct taxonomic mapping between isolates and dominant ASVs, the integration of culture-based and sequencing-based approaches provides complementary insights into community structure and functional potential. This combined framework enhances our understanding of microbial adaptation to recalcitrant polymers and supports the rational development of LDPE-targeted bioremediation strategies.

Biodegradation assays based on weight loss, FTIR, and SEM analyses were conducted. Apparent weight loss demonstrated clear isolate-dependent variation in LDPE degradation capacity, reflecting differences in metabolic potential, enzymatic systems, and surface colonization ability. The superior performance of *Bacillus* sp. K5 is consistent with previous reports (~21.6%) (Isha et al. 2024) and is likely associated with carbon-limited conditions that promote LDPE utilization, together with its broad repertoire of oxidative and hydrolytic enzymes, including laccases, peroxidases, and lipases (Harshvardhan and Jha 2013; Tirkey et al. 2025). *Microbacterium* isolates also exhibited substantial activity, in agreement with earlier studies demonstrating their ability to induce surface oxidation and polymer weight reduction. Differences between *M. aurantiacum* K2 and *Microbacterium* sp. K3 likely reflects strain-specific variation in enzyme expression, biofilm formation, and responses to environmental conditions (Sharma et al. 2022; Zhang et al. 2024).

Lower or intermediate degradation activities observed in *Brevibacterium*, *Aeromonas*, *Rhodococcus*, and *Brucella* isolates are consistent with previous reports linking polyethylene oxidation to biosurfactant production and strain-specific oxidative enzymes, including LMCO, AlkB, and monooxygenases (Alamer et al. 2023; Tao et al. 2023; Zhai et al. 2023). Control samples without bacterial inoculum showed 7.75% reduction, indicating that a portion of the observed mass loss may result from additive leaching, surface oxidation, or handling artefacts during film washing, drying, and preparations. Overall, variability in degradation efficiency reflects differences in enzymatic capacity, surface attachment, and metabolic activity, whereas minor mass loss in controls is attributable to additive leaching or abiotic oxidation rather than true biodegradation (Ghatge et al. 2020). Despite these potential non-biological contributions, the substantially higher mass loss in inoculated samples compared to controls demonstrates the relative contribution of microbial activity. Therefore, the data remain representative for evaluating the capacity of each isolate to promote LDPE apparent mass loss under the tested conditions. The three most active strains were selected for further structural and chemical analyses.

Detailed analyses were focused on the three most efficient isolates, namely *M. aurantiacum* K2, *Microbacterium* sp. K3, and *Bacillus* sp. K5. Gravimetric results indicated that LDPE degradation efficiency varied among isolates and was closely associated with their oxidative activity. FTIR analysis supported the gravimetric findings. The control, K2, and K3 samples did not exhibit distinct carbonyl (1700-1740 cm^{-1}) or hydroxyl (3200-3600 cm^{-1}) bands, resulting in negligible carbonyl and hydroxyl index values and indicating limited oxidative modification. In contrast, LDPE films incubated with *Bacillus* sp. K5 showed weak absorption bands at approximately 1654 cm^{-1} and 3462-3549 cm^{-1}, corresponding to carbonyl- and hydroxyl-related functional groups. Accordingly, K5 exhibited higher CI and HI values, suggesting the initiation of surface oxidation. The formation of oxygen-containing functional groups is characteristic of early-stage polyethylene biodegradation and may enhance surface polarity, facilitating microbial attachment and enzyme-substrate interactions. However, the absence of a pronounced carbonyl band near 1715 cm^{-1} indicates that advanced oxidation had not yet occurred.

The relatively higher performance of *Bacillus* sp. K5 may be related to its enzymatic versatility, as members of this genus are known to produce oxidative and hydrolytic enzymes involved in polymer modification (Harshvardhan and Jha 2013; Ojha et al. 2017). The persistent and dominant LDPE degradation by *Bacillus* in our study mirrors findings from Perdigão et al. (2026), where *Bacillus* strains were shown to have lipolytic activity, suggesting involvement of alternative degradation pathways. In contrast, LDPE samples are treated with *Microbacterium* sp. K3 and *M. aurantiacum* K2 showed negligible CI and HI values, consistent with their lower degradation efficiency. It should be noted that FTIR spectra were obtained without technical or biological replicates. Therefore, CI and HI values are presented descriptively, and statistical analysis

could not be performed. Future studies incorporating replicated measurements are required for a more robust quantitative evaluation.

SEM-EDS analysis was conducted to evaluate surface morphological and elemental changes in LDPE films following bacterial treatment. The control samples exhibited smooth, uniform, and intact surfaces with minimal defects, which is consistent with low crack area, low surface roughness, and high pore density values obtained from quantitative analysis. EDS spectra of the control were dominated by carbon with negligible oxygen content, indicating limited surface modification, in agreement with previous reports (Blair et al. 2019). LDPE films treated with *M. aurantiacum* K2 showed moderate surface alteration, characterized by mild roughening and shallow pits. These observations were supported by quantitative data showing moderate increases in crack area and surface roughness. EDS analysis revealed a slight increase in oxygen content relative to the control, suggesting measurable changes in surface elemental composition, consistent with earlier studies on microbial oxidation of polyethylene (Adamcová et al. 2018; Kotova et al. 2021).

Samples treated with *Microbacterium* sp. K3 exhibited more pronounced surface irregularities, including localized pits, grooves, and uneven cavities. Quantitative SEM analysis indicated higher crack area and surface roughness values compared to K2. Correspondingly, EDS spectra showed increased oxygen signals and traces of silicon, which have been previously associated with surface modification processes during microbial plastic weathering (Restrepo-Flórez et al. 2014; Tirkey et al. 2025). The most extensive morphological changes were observed in samples treated with *Bacillus* sp. K5, which displayed widespread microcracks, deep pits, and surface fragmentation. These features were consistent with the highest crack area, largest pit diameter, and highest roughness values among all treatments. EDS analysis showed relatively higher oxygen content and reduced carbon proportions compared to the control, indicating notable changes in surface elemental composition. These observations were further supported by FTIR results showing increased carbonyl and hydroxyl signals, as reported in similar biodegradation studies (Waqas et al. 2021).

Overall, the combined SEM, EDS, FTIR, and quantitative image analysis data demonstrate a progressive increase in surface modification from K2 to K3 and K5 treatments, which is consistent with the observed weight loss patterns. This trend supports previous findings on microbial polyethylene weathering and surface oxidation (Restrepo-Flórez et al. 2014; Muangchinda et al. 2024; Tirkey et al. 2025). However, it should be noted that surface features observed by SEM may also be influenced by environmental exposure, sample preparation, and handling procedures. Therefore, the detected morphological and elemental changes cannot be attributed solely to microbial activity. Nevertheless, the consistent trends observed across multiple analytical approaches support the association between bacterial treatment and surface modification.

The presence of LDPE-degrading bacteria in enrichment cultures derived from Pamekasan mangrove plastispheres indicates potential ecological relevance for plastic persistence and microbial dynamics in these environments. Mangrove ecosystems function as biodiversity hotspots, carbon sinks, and natural coastal barriers; however, increasing plastic accumulation in sediments and root systems poses substantial ecological risks, including physical smothering, altered sediment properties, and pollutant retention (Danso et al. 2019). Partial biodegradation mediated by plastisphere-associated bacteria may contribute to reducing the persistence and physical impacts of plastic debris on mangrove roots, benthic fauna, and sediment structure, potentially alleviating disruptions in oxygen diffusion and nutrient exchange over extended periods.

Plastisphere surfaces represent distinct ecological niches that selectively enrich taxa with oxidative metabolism and strong biofilm-forming capacity, including *Aeromonas*, *Bacillus*, *Microbacterium*, and *Rhodococcus*. This selective enrichment is consistent with the strain-specific variation in degradation efficiency discussed above and reflects differences in enzymatic activity, surface colonization, and metabolic adaptability. The formation of plastisphere biofilms and associated metabolic specialization has been widely recognized as a key factor influencing polymer transformation and community succession on plastic surfaces (Zettler et al. 2013; Danso et al. 2019). Given the central role of microbial communities in organic matter turnover and nutrient cycling in mangrove ecosystems, such compositional shifts may influence local biogeochemical processes depending on plastic load, residence time, and environmental conditions.

Although microbial colonization and partial degradation may reduce physical hazards associated with plastic debris, plastisphere biofilms may also facilitate the dispersal of opportunistic or non-native microorganisms (Zettler et al. 2013). The detection of genera containing potentially pathogenic species, such as *Aeromonas* and *Brucella*, highlights the need to evaluate ecological risks alongside biodegradation benefits, particularly under long-term or large-scale exposure scenarios. From a sustainability perspective, the occurrence of indigenous LDPE-degrading bacteria suggests an inherent ecosystem-based capacity for partial plastic attenuation. These microbial processes may support environmentally compatible bioremediation strategies, as in situ degradation avoids disturbances associated with mechanical removal or chemical treatments. However, microbial degradation alone cannot offset continuous plastic inputs and should be considered a complementary rather than standalone mitigation approach.

This study combines stepwise enrichment, ASV-resolved community analysis, and isolate-level functional validation to examine polyethylene degradation within a mangrove-derived plastisphere system. Previous studies have often addressed enrichment dynamics and single-isolate degradation assays separately, limiting direct comparison between community succession and functional performance. By integrating these approaches, the present results enable direct linkage between microbial community restructuring and LDPE degradation capacity. Earlier enrichment studies frequently reported pronounced biomass decline under recalcitrant substrates. In contrast, the observed marginal

reduction in cell density accompanied by substantial compositional shifts indicates that LDPE selection primarily operates through taxonomic replacement rather than biomass collapse, supporting its role as a selective ecological filter. Furthermore, variability in degradation efficiency among closely related taxa was associated with strain-level differences in oxidative metabolism, biofilm formation, and metabolic specialization, as reflected by consistent relationships between surface modification and weight loss.

The persistence of core ASVs throughout enrichment stages suggests the presence of metabolically flexible taxa that remain active during community restructuring. In addition, the sustained occurrence of *Aeromonas*, *Rhodococcus*, and *Brucella* indicates that LDPE-associated communities are not dominated exclusively by classical hydrocarbon degraders. Instead, the observed patterns are consistent with consortium-based degradation involving complementary metabolic functions. The persistence of *Bacillus* across enrichment stages, together with its dominant performance in degradation assays and consistent oxidative signatures, indicates that this genus represents a stable and functionally relevant member of LDPE-adapted communities rather than a transient opportunistic colonizer. The previous study indicates a consortium of bacteria, primarily *Pseudomonas*, *Bacillus*, and *Rhodococcus* capable of colonizing the "plastisphere" and degrading major polymers through specific enzymatic pathways (Barwant et al. 2026).

Despite these advances, several limitations should be acknowledged. First, the use of composite sediment samples and the absence of environmental measurements (e.g., salinity, pH, and temperature) limited statistical resolution and ecological interpretation. Future studies should incorporate spatially resolved sampling and concurrent environmental monitoring. Second, the lack of additional controls, such as inoculated carbon-free medium without LDPE and uninoculated LDPE incubations, constrained causal inference regarding LDPE-driven community shifts. Although logistical constraints prevented their inclusion, future experiments should incorporate these controls to strengthen validation. Third, FTIR analyses were conducted without replication, restricting quantitative interpretation of oxidation indices. Replicated spectroscopic measurements and complementary techniques are therefore required in future work. Fourth, degradation assessment based on mass loss, FTIR, and SEM-EDS reflects early to intermediate degradation stages and does not directly demonstrate complete mineralization. Future studies should integrate respirometric, isotope-labeling, and metabolite-based approaches to evaluate mineralization pathways. Finally, enrichment procedures likely favored fast-growing taxa, potentially underrepresenting slow-growing or syntrophic microorganisms. Cultivation-independent methods, consortium-based experiments, and multi-omics analyses should be applied to capture broader functional diversity.

In conclusion, this study shows that integrating stepwise enrichment, 16S rRNA amplicon sequencing, and isolate-level functional validation enables direct linkage between microbial community succession and LDPE degradation capacity under controlled conditions. The persistence of core taxa and the strain-specific variation in degradation performance indicate that LDPE transformation in mangrove-derived plastispheres is mediated by cooperative microbial processes rather than single dominant degraders, highlighting the potential of indigenous bacteria for environmentally compatible plastic attenuation. However, the observed degradation reflects early-stage processes and requires further validation under environmentally realistic conditions. Future studies should therefore focus on characterizing enzyme systems, examining consortium-level interactions, optimizing degradation conditions, and evaluating in situ performance to support the development of scalable bioremediation strategies.

ACKNOWLEDGEMENTS

The authors would like to express their sincere gratitude to the Graduate Program of Bioscience, Universitas Sebelas Maret, Indonesia, for providing laboratory facilities and technical support throughout this study. This research was funded by the Ministry of Higher Education, Science, and Technology in the 2025 fiscal year, through the thesis research grant with contract No 1186.1/UN27.22/PT.01.03/ 2025.

REFERENCES

Adamcova D, Radziemska M, Zloch J, Dvorackova H, Elbl J, Kynicky J, Brtnicky M, Vaverkova MD. 2018. SEM analysis and degradation behavior of conventional and bio-based plastics during composting. Acta Universitatis Agriculturae et Silviculturae Mendelianae Brunensis 66 (2): 349-356. https://doi.org/10.11118/actaun201866020349.

Agostini L, Moreira JCF, Bendia AG, Kmit MCP, Waters LG, Santana MFM, Sumida PYG, Turra A, Pellizari VH. 2021. Deep-sea plastisphere: Long-term colonization by plastic-associated bacterial and archaeal communities in the Southwest Atlantic Ocean. Sci Total Environ 793: 148335. https://doi.org/10.1101/2021.01.26.428295.

Alamer NJ, Aldayel MF, Khalifa A. 2023. Isolation and characterization of *Brucella* spp., low-density polyethylene (LDPE) plastic degrading bacteria in Al-Ahsa region, Saudi Arabia. Appl Sci 13 (7): 4629. https://doi.org/10.3390/app13074629.

Barwant MM, Ali UM, Tolani TR. 2026. Microplastic pollution in aquatic environments: A systematic review of bacterial degradation efficacy, mechanisms, and future pathways. Front Earth Sci 14: 1752600. https://doi.org/10.3389/feart.2026.1752600.

Blair RM, Waldron S, Phoenix VR, Gauchotte-Lindsay C. 2019. Microscopy and elemental analysis characterisation of microplastics in sediment of a freshwater urban river in Scotland, UK. Environ Sci Pollut Res 26: 12491-12504. https://doi.org/10.1007/s11356-019-04678-1.

Bocci V, Galafassi S, Levantesi C, Crognale S, Amalfitano S, Congestri R, Matturo B, Rossetti S, Pippo FD. 2024. Freshwater plastisphere: A review on biodiversity, risks, and biodegradation potential with implications for the aquatic ecosystem health. Aquat Microbiol 15: 1395401. https://doi.org/10.3389/fmicb.2024.1395401.

Cordova MR, Ulumuddin YI, Lubis AA, Kaisupy MT, Wibowo SPA, Subandi R, Yogaswara D, Purbonegoro T, Renyaan J, Nurdiansah D, Sugiharto U, Shintianata D, Meiliastri SS, Andini FP, Suratno, Ilman M, Anggoro AW, Basir, Cragg SM. 2023. Microplastics leaving a trace in mangrove sediments ever since they were first manufactured: A study from Indonesia mangroves. Mar Pollut Bull 195: 115517. https://doi.org/10.1016/j.marpolbul.2023.115517.

Dang H, Ewald JM, Mattes TE. 2023. Genome-resolved metagenomics and metatranscriptomics reveal insights into the ecology and

metabolism of anaerobic microbial communities in PCB-contaminated sediments. Bioremediat Biotechnol 57 (43): 16386-16398. https://doi.org/10.1021/acs.est.3c05439

Danso D, Chow J, Streit WR. 2019. Plastics: Environmental and biotechnological perspectives on microbial degradation. Appl Environ Microbiol 81 (19): e01095-19. https://doi.org/10.1128/AEM.01095-19.

Deakin K, Porter A, Baquero AO, Lewis C.2025. Plastic pollution in mangrove ecosystems: A global meta-analysis. Mar Pollut Bull 218: 1-14. https://doi.org/10.1016/j.marpolbul.2025.118165.

Dhali SL, Parida D, Kumar B, Bala K. 2024. Recent trends in microbial and enzymatic plastic degradation: A solution for plastic pollution predicaments. Biotechnol Sustain Mater 1 (11): 1-23. https://doi.org/10.1186/s44316-024-00011-0.

Geyer R, Jambeck JR, Law KL. 2017. Production, use, and fate of all plastics ever made. Sci Adv 3 (7): e1700782. https://doi.org/10.1126/sciadv.1700782.

Ghatge S, Yang Y, Ahn JH, Hur H. 2020. Biodegradation of polyethylene: A brief review. Appl Biol Chem 63: 27. https://doi.org/10.1186/s13765-020-00511-3.

Goraj W, Pytlak A, Grzadziel J, Galazka A, Stepniewska Z, Szafranek-Nakonieczna A. 2023. Dynamics of methane-consuming biomes from Wieliczka Formation: Environmental and enrichment studies. Biology 12 (11): 1420. https://doi.org/10.3390/biology12111420.

Hardoim CCP, Cardinale M, Cúcio ACB, Esteves AIS, Berg G, Xavier JR, Cox CJ, Costa R. 2014. Effects of sample handling and cultivation bias on the specificity of bacterial communities in keratose marine sponges. Front Microbiol 5: 611. https://doi.org/10.3389/fmicb.2014.00611.

Harshvardhan K, Jha B. 2013. Biodegradation of low-density polyethylene by marine bacteria from pelagic waters, Arabian Sea, India. Mar Pollut Bull 77: 100-106. https://doi.org/10.1016/j.marpolbul.2013.10.025.

Isha, Ali S, Chang YC. 2024. Biodegradation of polyethylene using *Bacillus tropicus* isolated from sewage wastewater treatment plant. Processes 12 (11): 2516. https://doi.org/10.3390/pr12112516.

Kato S, Goya E, Tanaka M, Kitagawa W, Kikuchi Y, Asano K, Kamagata Y. 2016. Enrichment and isolation of *Flavobacterium* strains with tolerance to high concentrations of cesium ion. Sci Rep 6: 20041. https://doi.org/10.1038/srep20041.

Kimber RL, Elizondo G, Jedyka K, Boothman C, Cai R, Bagshaw H, Haigh SJ, Coker VS, Lloyd JR. 2023. Copper bioreduction and nanoparticle synthesis by an enrichment culture from a former copper mine. Environ Microbiol 25 (12): 3139-3150. https://doi.org/10.1111/1462-2920.16488.

Kotova IB, Taktarova YV, Tsavkelova EA, Egorova MA, Bubnov IA, Malakhova DV, Shirinkina LI, Sokolova TG, Bonch-Osmolovskaya EA. 2021. Microbial degradation of plastics and approaches to make it more efficient. Microbiology 90: 671-701. https://doi.org/10.1134/S0026261721060084.

Jiao S, Chen W, Wang E, Wang J, Liu Z, Li Y, Wei G. 2016. Microbial succession in response to pollutants in batch-enrichment culture. Sci Rep 6: 21791. https://doi.org/10.1038/srep21791.

Lehr K, Oosterlinck B, Then CK, Gemmell MR, Gedgaudas R, Bornschein J, Kupcinskas J, Smet A, Hold G, Link A, ENIGMA: European Network for the Investigation of Gastrointestinal Mucosal Alterations. 2025. Comparison of different microbiome analysis pipelines to validate their reproducibility of gastric mucosal microbiome composition. mSystems 10 (2): e0135824. https://doi.org/10.1128/msystems.01358-24.

Li Z, Wei R, Gao M, Ren Y, Yu B, Nie K, Xu H, Liu L. 2020. Biodegradation of low-density polyethylene by *Microbulbifer hydrolyticus* IRE-31. J Environ Manag 263: 110345. https://doi.org/10.1016/j.jenvman.2020.110345.

Ligo A, Juliandi MD, Agustien A, Djamaan A. 2020. Isolation and characterization of polyethylene-degrading marine bacteria. J Pharm Biol Sci 15 (6): 22-25. https://doi.org/10.9790/3008-1506032225.

Madhuri RJ, Saraswathi M, Gowthami K, Bhargavi M, Divya Y, Deepika V. 2019. Recent approaches in the production of novel enzymes from environmental samples by enrichment culture and metagenomic approach. Recent Dev Appl Microbiol Biochem 19: 251-262. https://doi.org/10.1016/B978-0-12-816328-3.00019-2.

Mishra S, Dash D, Das AP. 2023. Aquatic microbial diversity on plastisphere: Colonization and potential role in microplastic biodegradation. Geomicrobiol J 41 (4): 312-323. https://doi.org/10.1080/01490451.2023.2242724.

Mohanan N, Montazer Z, Sharma PK, Levin DB. 2020. Microbial and enzymatic degradation of synthetic plastics. Front Microbiol 11: 580709. https://doi.org/10.3389/fmicb.2020.580709.

Moharir RV, Kumar S. 2019. Challenges associated with plastic waste disposal and allied microbial routes for its effective degradation: A comprehensive review. J Clean Prod 208: 65-76. https://doi.org/10.1016/j.jclepro.2018.10.059.

Montazer Z, Habibi Najafi MB, Levin DB. 2020. Challenges with verifying microbial degradation of polyethylene. Polymers 12: 123. https://doi.org/10.3390/polym12010123.

Muangchinda C, Pinyakong O. 2024. Enrichment of LDPE-degrading bacterial consortia: Community succession and enhanced degradation efficiency through various pretreatment methods. Sci Rep 14: 28795. https://doi.org/10.1038/s41598-024-80306-4.

Muthukumar N, Mohanan S, Maruthamuthu S, Subramanian P, Palaniswamy N, Raghavan M. 2003. Role of *Brucella* sp. and *Gallionella* sp. in oil degradation and corrosion. Electrochem Commun 5 (5): 421-425. https://doi.org/10.1016/S1388-2481(03)00093-6.

Ojha N, Pradhan N, Singh S, Barla A, Shrivastava A, Bose S, Rai V. 2017. Evaluation of HDPE and LDPE degradation by fungus, *Bacillus* and *Stenotrophomonas* species. Environ Dev Sustain 19 (4): 1151-1167. https://doi.org/10.1007/s10668-016-9843-4.

Parida D, Katare K, Ganguly A, Chakraborty D, Konar O, Noguiera R, Bala K. 2024. Molecular docking and metagenomics assisted mitigation of microplastic pollution. Chemosphere 351: 141271. https://doi.org/10.1016/j.chemosphere.2024.141271.

Pawano O, Jenpuntarat N, Streit WR, Pérez-García P, Pongtharangkul T, Phinyocheep P, Thayanukul P, Euanorasetr J, Intra B. 2024. Exploring untapped bacterial communities and potential polypropylene-degrading enzymes from mangrove sediment through metagenomics analysis. Front Microbiol 15: 1347119. https://doi.org/10.3389/fmicb.2024.1347119.

Perdigão R, Alexandrino DA, Carvalho MF, Magalhães C, Almeida CM, Mucha AP. 2026. Genome mining and screening for plastic-degrading potential in marine bacteria. Appl Microbiol Biotechnol 110: 87. https://doi.org/10.1007/s00253-026-13767-4.

Pinto Y, Bhatt AS. 2024. Sequencing-based analysis of microbiomes. Nat Rev Genet 25: 829-845. https://doi.org/10.1038/s41576-024-00746-6.

Restrepo-Flórez JM, Bassi A, Thompson MR. 2014. Microbial degradation and deterioration of polyethylene - A review. Intl Biodeterior Biodegrad 88: 83-90. https://doi.org/10.1016/j.ibiod.2013.12.014.

Rodriguez-Pazmiño AS, Carvajal E, Paredes-Núñez D, Echeverría J, Calderon J, Orlando SA, Parra Vera H, Garcia-Bereguiain MA. 2025. Comparative evaluation of MALDI-ToF mass spectrometry and Sanger sequencing of the *16S*, *hsp65*, and *rpoB* genes for non-tuberculous mycobacteria species identification. Front Cell Infect Microbiol 15: 1612459. https://doi.org/10.3389/fcimb.2025.1612459.

Rong Z, Ding ZH, Wu YH, Xu XW. 2024. Degradation of low-density polyethylene by the bacterium *Rhodococcus* sp. C-2 isolated from seawater. Sci Total Environ 907: 167993. https://doi.org/10.1016/j.scitotenv.2023.167993.

Salinas J, Carpena V, Martínez-Gallardo MR, Segado M, Estrella-González MJ, Toribio AJ, Jurado MM, López-González JA, Suárez-Estrella F, López MJ. 2023. Development of plastic-degrading microbial consortia by induced selection in microcosms. Front Microbiol 14: 1143769. https://doi.org/10.3389/fmicb.2023.11sevi43769.

Sharma S, Mathur N, Singh A, Agarwal M. 2022. Biodegradation of low- and high-density polyethylene films by *Microbacterium barkeri* SH20. Curr World Environ 17 (1): 245-254. https://doi.org/10.12944/CWE.17.1.22.

Sheng Y, Ye X, Zhou Y, Li R. 2021. Microplastics (MPs) act as sources and vector of pollutants-impact hazards and preventive measures. Bull Environ Contam Toxicol 107 (4): 722-729. https://doi.org/10.1007/s00128-021-03226-3.

Singh J, Shah A, Parmar H, Duttaroy B. 2025. Bacteriological profile and antibiotic susceptibility patterns in lower respiratory tract infection at a tertiary care teaching hospital. GAIMS J Med Sci 5 (1): 167-174. https://doi.org/10.5281/zenodo.14788464.

Skariyachan S, Taskeen N, Kishore AP, Krishna BV, Naidu G. 2021. Novel consortia of *Enterobacter* and *Pseudomonas* formulated from cow dung exhibited enhanced biodegradation of polyethylene and polypropylene. J Environ Manag 284: 112030. https://doi.org/10.1016/j.jenvman.2021.112030.

Silva AL, Prata JC, Duarte AC, Soares AM, Barceló D, Rocha-Santos T. 2021. Microplastics in landfill leachates: The need for reconnaissance studies and remediation technologies. Case Stud Chem Environ Eng 3: 100072. https://doi.org/10.1016/j.cscee.2020.100072.

Smith SD. 2012. Marine debris: A proximate threat to marine sustainability in Bootless Bay, Papua New Guinea. Mar Pollut Bull 64 (9): 1880-1883. https://doi.org/10.1016/j.marpolbul.2012.06.013.

Tao X, Ouyang H, Zhou A, Wang D, Matlock H, Morgan JS, Ren AT, Mu D, Pan C, Zhu X, Han A, Zhou J. 2023. Polyethylene degradation by a *Rhodococcus* strain isolated from naturally weathered plastic waste enrichment. Environ Sci Technol 57 (37): 13901-13911. https://doi.org/10.1021/acs.est.3c03778.

Tirkey A, Upadhyay LSB. 2025. Introducing the LDPE degrading microbes of sedimentary systems: From dumpsite to laboratory. Environ Sci Adv 4: 952-963. https://doi.org/10.1039/D5VA00058.

UNEP. 2021. From pollution to solution: A global assessment of marine litter and plastic pollution reveals the impact of marine litter and plastic pollution in the environment and their effects on the health of ecosystems, wildlife and humans. UNEP, Nairobi. https://www.unep.org/interactives/beat-plastic-pollution/?gad_source=1&gclid=Cj0KCQiAsaS7BhDPARIsAAX5cSDp006VFGXGyTfihzyGjgxiHpjXTBkfkgYZHGINl4l7eizlUFl01ScaAmvSEALw_wcB. [24 December 2024]

Wang J, Zhao X, Wu A, Tang Z, Niu L, Wu F, Wang F, Zhao T, Fu Z. 2021. Aggregation and stability of sulfate-modified polystyrene nanoplastics in synthetic and natural waters. Environ Pollut 268: 114240. https://doi.org/10.1016/j.envpol.2020.114240.

Wang M, Noor S, Huan R, Liu C, Li JY, Shi Q, Zhang YJ, Wu C, He H. 2020. Comparison of the diversity of cultured and total bacterial communities in marine sediment using culture-dependent and sequencing methods. PeerJ 8: e10060. https://doi.org/10.7717/peerj.10060.

Waqas M, Haris M, Asim N, Islam HU, Abdullah A, Khan A, Khattak H, Waqas M, Ali S. 2021. Biodegradable potential of *Bacillus amyloliquefaciens* and *Bacillus safensis* using low density polyethylene thermoplastic (LDPE) substrate. Eur J Environ Public Health 5 (2): em0069. https://doi.org/10.21601/ejeph/9370.

Waymire E, Samake JN, Gunarathna I, Carter TE. 2024. A decade of invasive *Anopheles stephensi* sequence-based identification: Toward a global standard. Trends Parasitol 4 (6): 477-486. https://doi.org/10.1016/j.pt.2024.04.012.

Wicaksono JA, Purwadaria T, Yulandi A, Tan WA. 2022. Bacterial dynamics during the burial of starch-based bioplastic and oxo-low-density-polyethylene in compost soil. BMC Microbiol 22: 309. https://doi.org/10.1186/s12866-022-02729-1.

Williams AT, Rangel-Buitrago N. 2022. The past, present, and future of plastic pollution. Mar Pollut Bull 176: 113429. https://doi.org/10.1016/j.marpolbul.2022.113429.

Wright RJ, Bosch R, Langille MGI, Gibson MI, Christie-Oleza JA. 2021. A multi-OMIC characterisation of biodegradation and microbial community succession within the PET plastisphere. Microbiome 9: 141. https://doi.org/10.1186/s40168-021-01054-5.

Zeenat, Elahi A, Bukhari DA, Shamim S, Rehman A. 2021. Plastics degradation by microbes: A sustainable approach. J King Saud Univ Sci 33 (6): 101538. https://doi.org/10.1016/j.jksus.2021.101538.

Zettler ER, Mincer TJ, Amaral-Zettler LA. 2013. Life in the "plastisphere": Microbial communities on plastic marine debris. Environ Sci Technol 47 (13): 7137-7146. https://doi.org/10.1021/es401288x.

Zhai X, Zhang XH, Yu M. 2023. Microbial colonization and degradation of marine microplastics in the plastisphere: A review. Front Microbiol 14: 1127308. https://doi.org/10.3389/fmicb.2023.1127308.

Zhang T, Li X, Rao X, Peng Y, Zhao C, Xu Y, Li J, Wei J. 2024. Biodegradation of polystyrene and polyethylene by *Microbacterium esteraromaticum* SW3 isolated from soil. Ecotoxicol Environ Saf 274: 1-9. https://doi.org/10.1016/j.ecoenv.2024.116207.